Surface & Coatings Technology 204 (2010) 2944–2949

Contents lists available at ScienceDirect

Surface & Coatings Technology

journal homepage: www.elsevier.com/locate/surfcoat

# Nanomechanical properties of bioactive films grown on low energy ion implanted Ti

Gelson Biscaia de Souza [a,*], Gabriel Goetten de Lima [b], Carlos Maurício Lepienski [b], Carlos Eugênio Foerster [c], Neide Kazue Kuromoto [b]

[a] Departamento de Ciências, Universidade Estadual de Maringá, CEP 87020-900, Maringá, PR, Brazil
[b] Departamento de Física, Universidade Federal do Paraná, CP 19044, CEP 81531-990, Curitiba, PR, Brazil
[c] Departamento de Física, Universidade Estadual de Ponta Grossa, CEP 84030-900, Ponta Grossa, PR, Brazil

ARTICLE INFO

Available online 6 February 2010

*Keywords:*
Glow discharge
Titanium
Bioactivity
Thin film
Instrumented indentation
Nanoscratch

ABSTRACT

Surface modification processes such as the alkali-heat treatment (AHT) can be employed in order to improve the titanium osseointegration with living tissues. Sodium titanate films produced by AHT presented high *in vitro* bioactivity when soaked in simulated body fluid. In order to produce bioactive surfaces and also improve the tribo-mechanical response of AHT films grown on Ti, samples were submitted to H, N and O low energy ion implantation (glow discharge—GD) at different working conditions. AHT film with thickness of 1 μm was produced on untreated Ti and had low hardness (0.012 GPa) as well as low critical nanoscratch resistance (5.5 mN). For the studied periods up to 30 days no *in vitro* bioactivity was observed on the only GD worked surfaces. Hydrogenated and nitrided Ti became bioactive after the AHT, but the film thickness decreases in comparison to untreated GD Ti. At the same time its critical nanoscratch resistance and bioactivity degree decrease. However for GD oxidized sample an AHT film was not formed. From these results it can be suggested that plenty availability of metallic Ti at the surface is required to grow AHT films with good bioactivity response.



## 1. Introduction

Surface treatment of titanium devices in alkali solutions has been presented as an effective method to induce bioactivity on these materials [1,2]. The chemical reactions produce sodium titanate films of about 1 μm thick, which in the presence of physiological or simulated body fluids (SBF), become negatively charged due to the formation of hydroxyl groups. This condition allows calcium phosphate precipitation on Ti surface resulting in an osseointegration with living tissues. Another way to induce the Ti bioactivity is the ion implantation of selected ionic species [3–7]. Plasma-based ion implantations (PBII) of calcium, sodium, water and hydrogen on titanium (energies ~10 keV) have presented good results for *in vitro* cytocompatibility and also the precipitation of calcium phosphate in SBF. As well as in the alkali treatment, the hydroxyl groups, formed right after the PBII and/or by ion exchanging with body fluids, contribute to the observed bioactivity of the PBII-treated Ti.

Mechanical features of the modified surfaces are very important parameters to be considered in biomedical implants [8]. The loading transference between bodies in contact rules the implant stability and its long-term use. Moreover, the surface modifications must be preserved after the surgery procedure, which involves screwing and shearing, e.g., as fixing maxillary screws. A suitable technique to improve mechanical and tribological responses of materials surface is the glow discharge (GD), which employs low ion energies (<1 keV) [9]. There is a lack of information concerning GD use to promote bioactive surfaces. In the present study, we performed hydrogenation, nitriding and oxidizing by GD on Ti. After that, alkali-heat treatment (AHT) was employed in order to induce bioactivity on the modified surfaces. The bioactivity was evaluated by using SBF solution and the mechanical and tribological properties by instrumented indentation.

## 2. Experimental procedure

Samples of cp-Ti (grade 2) were cut into 1 cm × 1 cm × 0.2 cm plates. A mirror-like surface finishing (average roughness $R_a = 18$ nm) was obtained by colloidal silica suspension polishing.

The DC glow discharge working parameters are presented in Table 1. The $H_2$, $N_2$ and $O_2$ are typical atmospheres employed in DC glow discharge treatments, and the modifications produced by them can become the Ti surface bioactive (specially oxidizing and hydrogenation) [1]. The temperature was controlled by monitoring a backside thermocouple and adjusting the plasma current as needed. The hydrogenation process was performed at 150 °C because this temperature corresponds to the upper limit to sustain the discharge. The temperatures of 500 °C and 600 °C for oxidation and nitriding, respectively, were employed in order to produce thick modified layers with low roughness degree [9].

* Corresponding author. Tel.: +55 44 3522 1851.
*E-mail address:* gbsouza@uem.br (G.B. de Souza).

0257-8972/$ – see front matter © 2010 Elsevier B.V. All rights reserved.
doi:10.1016/j.surfcoat.2010.02.010

**Table 1**
Treatment conditions of the low energy ion implanted samples.

| Sample | Atmosphere | Temperature (°C) | Time (h) | Current (mA) | Tension (V) | Pressure ($10^2$ Pa) |
|---|---|---|---|---|---|---|
| Hydrogenated | 100% $H_2$ | 150 | 3 | 60 | 400 | 5.1 |
| Nitrided | 60% $N_2$ 40% $H_2$ | 600 | 3 | 350 | 510 | 4.6 |
| Oxidized | 100% $O_2$ | 480 | 3 | 260 | 480 | 2.1 |

The AHT was performed according to the protocol described in [1,2]. The samples were immersed in 5 M NaOH solution during 24 h at 60 °C. After that, they were ramp heated (5 °C/min) up to 600 °C, kept at this temperature during 1 h and then cooled to room temperature.

Bioactivity was evaluated by using SBF prepared according to the Kokubo and Takadama [10] recipe and suggested routine, which is widely reported in the literature. The samples were soaked in SBF during 14, 19, 28 and 30 days at 36.5 ± 0.5 °C. At each four days the SBF solution was renewed. In order to identify surface structural modifications, X-ray diffraction (XRD) using Cu $K_\alpha$ radiation in Bragg–Brentano geometry and thin film XRD (TF-XRD) at grazing incidence of $\alpha = 1°$ were employed. Surface morphologies were observed by scanning electron microscopy (SEM) along with electron dispersive X-ray spectroscopy (EDS) to observe the elemental composition.

Hardness and elastic modulus profiles were obtained by instrumented indentation following the Oliver–Pharr method [11]. The applied loads ranged from 0.14 mN to 300 mN and the tip was a Berkovich type diamond indenter. The nanoscratch tests were performed by the instrumented indentation device using the same tip. The ramping load ranged from 50 μN to 10 mN following the tip edge direction.

## 3. Results and discussion

### 3.1. Structural features, surface morphology and bioactivity

Fig. 1 shows XRD patterns of (a) Ti treated by GD processes and (b) after that submitted to AHT. As can be observed in Fig. 1a, the GD processes produced TiH, titanium nitrides and oxides after hydrogenation, nitriding and oxidizing, respectively. For the oxidizing process rutile (R) and anatase (A) phases were also identified. A reflection in approximately 37.7°, adjacent to the Ti peak, marked with an asterisk, may correspond to the substoichiometric phase $TiN_{0.3}$. This compound can be formed in reactive process of Ti with N, since it has been reported for TiN films, laser nitriding, and N-ion implanted Ti [12–14]. Because the alkali treatment produces thin films of sodium titanate on the Ti surface, X-ray grazing incidence in the samples after the AHT was performed. Fig. 1b shows that the AHT on untreated GD Ti produced sodium titanate (N) (peaks at 24°, 28° and 48°) and rutile, in accordance with literature data [1,15,16]. Regarding the previously hydrogenated and nitrided samples, the N peaks decreased in intensity, and the peak at 48° is the most evident. As a general observation, the N diffraction peaks are broad, indicating a low crystallinity and/or a slight variation on its stoichiometry. Additionally, the compound $TiN_{0.3}$ can be better indexed in this TF-XRD geometry condition. However, in the AHT oxidized sample (not here shown), diffraction pattern did not show significant differences in comparison to the only oxidized sample. This means that none of the sodium titanate peaks could be indexed.

Fig. 2 shows typical micrographs of the surface morphology after AHT in (a) untreated and in GD samples: (b) hydrogenated, (c) nitrided, and (d) oxidized. These micrographs disclose a typical microporous structure for the AHT thin films [1,15–17]. It is also observed that the pore size decreases from untreated to hydrogenated and nitrided samples. This observation can be attributed to a film growing kinetics

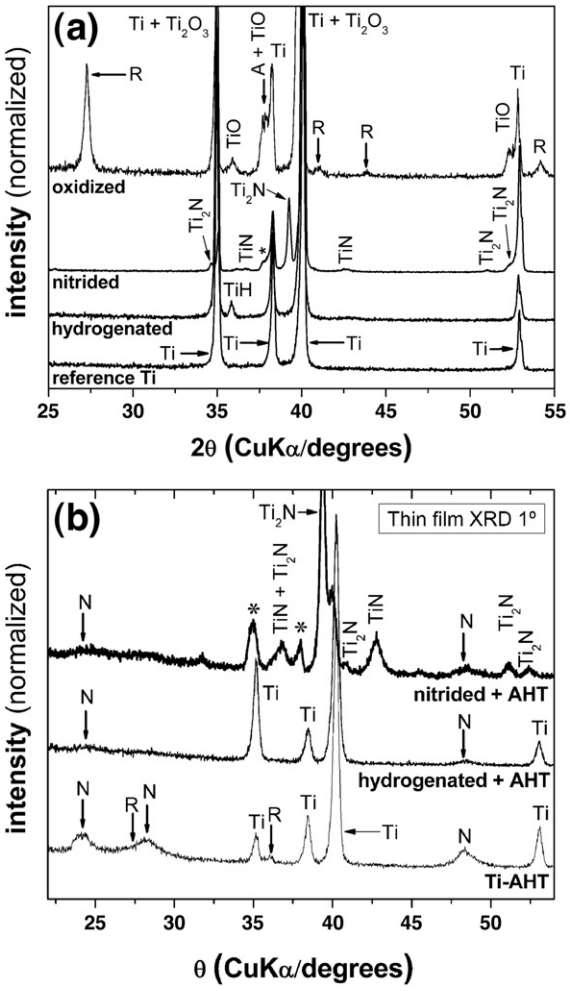


**Fig. 1.** X-ray diffraction patterns. (a) GD samples at Bragg–Brentano geometry. (b) Grazing incidence (TF-XRD) of the GD samples after AHT. Peaks indicated with (*) are suggested to be the substoichiometric phase $TiN_{0.3}$. A = anatase; R = rutile; N = sodium titanate.

that depends on the previous GD process. Moreover, as observed in Fig. 2d, the previous oxidized sample did not show the presence of sodium titanate film after the AHT, indicating morphology identical to the only oxidized sample. The absence of AHT film on the oxidized sample is in agreement with the TF-XRD patterns.

In order to verify the effect of GD and GD plus AHT processes on the surface bioactivity, *in vitro* SBF essays were performed. According to Kokubo and Takadama [10], by these essays hydroxyapatite (HA) can nucleate on surfaces which present adequate conditions for bioactivity. Moreover, the degree of HA formation is indicative of the bioactivity degree, that is, a material able to form it in a short period will bond to living bone in a short period, by means of the HA nucleation in the living body. SEM, EDS and TF-XRD analyses showed that samples only GD worked, as well as untreated Ti did not present *in vitro* bioactivity for the studied periods of 14, 19, 28 and 30 days. On the other hand, if AHT is performed the surfaces became bioactive, as verified by the nucleation of HA on them. On the GD oxidized sample plus AHT, which not presented sodium titanate film, nucleation of any kind was identified. Fig. 3 shows typical SEM images of surfaces (untreated and GD worked plus AHT) soaked during 19 days in SBF solution. Fig. 3a shows an effective hydroxyapatite layer grown on the Ti only submitted to AHT, as verified by TF-XRD analysis. Moreover, EDS analyses indicated a Ca/P ratio of 1.67 ± 0.06, which corresponds to crystalline HA correspondent to the stable calcium phosphate phase in the body [1,18]. The film fractures observed in this image are due to water loss during the acquisition of the SEM images.

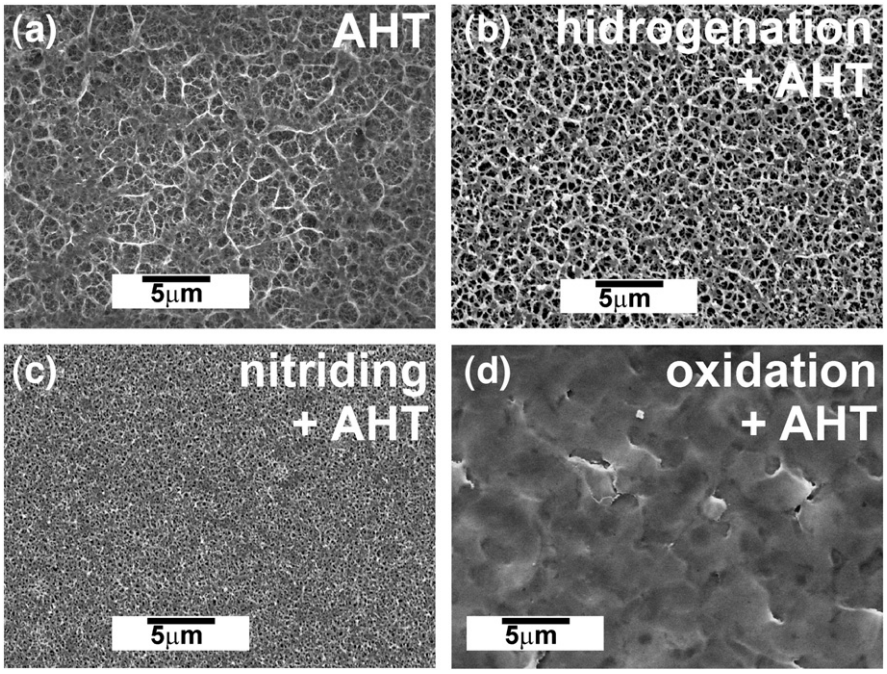


**Fig. 2.** Micrographs (SEM) of titanium surfaces submitted to GD and after to AHT: (a) untreated; (b) hydrogenated; (c) nitrided; (d) oxidized.

In Fig. 3b–c typical HA nuclei obtained on GD plus AHT samples are shown. Instead a layer now is formed in dispersed HA nuclei. The sodium titanate film is still present on these samples. EDS analyses (Fig. 3d) of these nuclei indicated a Ca/P ratio of $1.45 \pm 0.26$ that corresponds to amorphous calcium phosphates [18]. SEM images of samples after additional soaking periods (not here shown) did not indicate significant increase in HA nuclei amount and sizes.

### 3.2. Mechanical properties

According to the literature [2,16,17,19] typical thicknesses of AHT layer grown on Ti in the same conditions here employed are in the range of 1 to 1.5 μm. The AHT films produced in the present work were better identified by using TF-XRD, and this fact suggests similar film thickness as reported in the literature. As a consequence, the study of

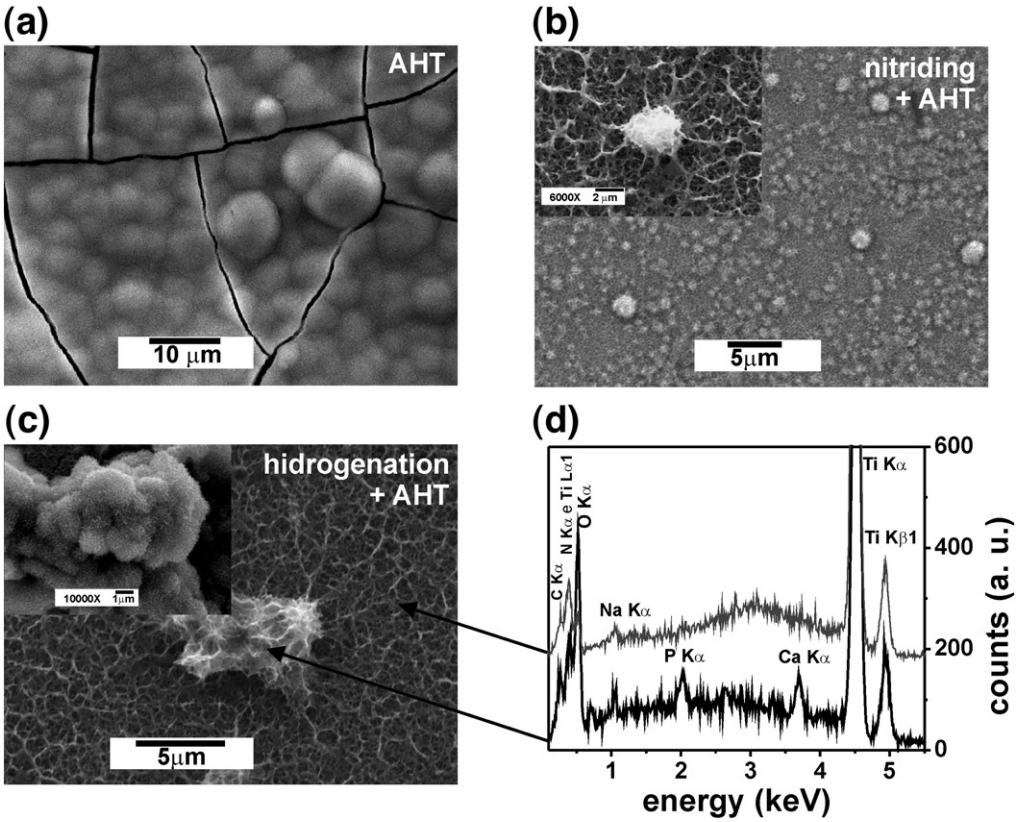


**Fig. 3.** Micrographs (SEM) of titanium surfaces submitted to GD and AHT, after immersion in SBF for 19 days: (a) untreated; (b) nitrided; (c) hydrogenated. (d) EDS spectra of regions indicated in (c). The insets in micrographs correspond to detail magnifications.

the mechanical properties should consider a thin modified layer on a substrate. In this case, the film hardness can be determined only if the penetration depth is lower than 10% of the film thickness since for higher depths the substrate affects the measured hardness [20–22]. In respect to the elastic modulus, even for very low penetration depths, the measured values are influenced by the substrate because the elastic deformation field has a wide range than the plastic one [20].

Fig. 4 summarizes hardness profiles for the different Ti modified surfaces which, after AHT, promoted the bioactive film growing. The untreated Ti has its hardness increased at near surface due to varied effects: indentation size effect, mechanically induced surface hardening, stresses produced by the mechanical polishing and surface oxides [11]. As expected the GD processes on Ti increase the near surface hardness for the nitrided samples (from 3.5 to 10 GPa at 200 nm in depth). Hydrogenated sample had similar hardness profiles in respect to the untreated GD condition. Significant differences on hardness profile shapes occur after the AHT: *(a)* the hardness at the near surface region is lower than the substrate; *(b)* the profiles are GD process dependent. Such hardness behavior is typical of soft films on hard substrates [20–22], in which the composite nature of the modified region (film plus substrate) produces profiles that continuously increase from low values (close to the film one) towards the substrate value. According to studies conducted by Tsui and Pharr [21] and Saha and Nix [22], the loading/unloading and hardness versus penetration depth responses for the composite show an inflection point when the penetration surpasses the film thickness, since the substrate effects become more significant. Based on these statements, analyses of loading/unloading curves allowed estimating that the film grown on the Ti only submitted to AHT has a thickness of about 1 μm, which is in accordance to the literature [2,16,17,19]. This thickness was determined by comparing curve shapes of Ti and Ti plus AHT film. Moreover, in Fig. 4 the untreated Ti plus AHT hardness profile presents an increase on its derivative at ~1 μm in depth, as expected according to the aforementioned studies [21,22]. The same procedure was made in the other GD samples and the films are thinner as shown in Table 2. In spite of the rise in the hardness profiles for the AHT hydrogenated and nitrided surfaces, we attribute the increase on hardness to the diminishing film thickness since the substrate contribution to hardness becomes higher [20–22]. Based on the above statement it is possible to estimate from sample Ti plus AHT film that the film hardness is about 20 MPa, obtained at the lowest applied load (0.15 mN). At this same load, the measured elastic modulus was about 3 GPa.

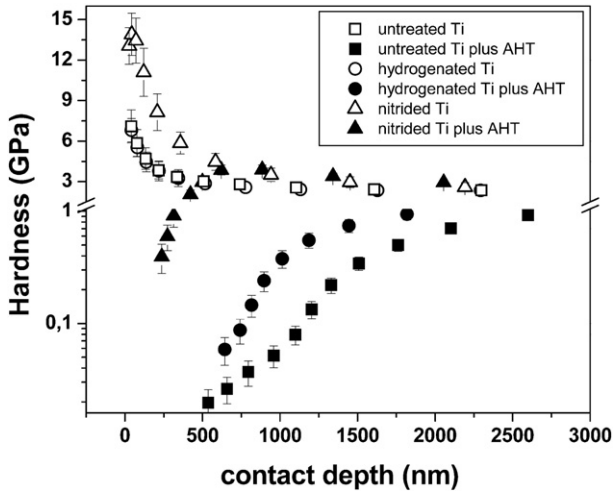


**Fig. 4.** Hardness profiles for titanium surfaces submitted to GD, before (open symbols) and after (closer symbols) the AHT film growing.

**Table 2**
Thickness and critical scratch resistance load of sodium titanate films produced on titanium submitted to GD and subsequent AHT.

| Sample | Film thickness (nm) | Critical scratch resistance load (mN) |
|---|---|---|
| Ti-AHT | 1029 ± 76 | 5.5 |
| Hidrogenated + AHT | 557 ± 70 | 2.7 |
| Nitrided + AHT | 202 ± 37 | 0.6 |
| Oxidized + AHT | Zero | – |

### 3.3. Nanoscratch

Fig. 5 shows SEM images of selected nanoscratch track regions for untreated Ti and the AHT films produced on it and on GD worked Ti surfaces. The inset in the upper left corner indicates the load progress during scratching. Images a–d show the region of nanoscratches at the applied load of 50 μN for untreated Ti, Ti plus AHT, hydrogenated Ti plus AHT and nitrided Ti plus AHT, respectively. No scratch damage is observed on untreated Ti while after AHT the tip track indicated film crushing. On the other hand, in films on samples previously GD worked, less crushing is observed and the scratch shape is narrower and sharper. By increasing the tip load during the scratch test, it was possible to observe the film cutting process until reaching the Ti substrate. Fig. 5e–h show the 5 mN scratch region. For samples GD worked the film is now surpassed, showing the substrate below, while for Ti only submitted to AHT some film still remains, but damaged. The scratch tracks were EDS scanned and a critical scratch resistance (when no film remains track inside), was determined and shown in Table 2.

As reported in the literature [10], a surface presents bioactivity when HA is nucleated on it after soaking periods in SBF. Our results indicate that GD processes, when employed alone and at the studied conditions, are not able to promote *in vitro* bioactivity on Ti surfaces. These results are somehow different from the ones reported by Xie et al. [5], who performed water and hydrogen implantations by plasma immersion ion implantation (PIII) on Ti. The authors attributed the observed *in vitro* bioactivity to the increase in the amount of hydroxyl radicals, which will start the HA nucleation in SBF. According to several authors [1–5], the hydroxyl formation is a key requirement for the titanium bioactivity in the SBF environment. However, in our study using GD, we attribute the absence of *in vitro* bioactivity to the employed low energy process. It is possible that low energy ions promote more ballistic effects (atomic displacements) than ionizations on Ti surface [23]. Thus, the low energy process (GD) does not make available a sufficient amount of free hydroxyl radicals in comparison to higher ion energies.

A characteristic behavior of the AHT film growing on titanium can be inferred from the GD plus AHT combination. The alkali treatment is currently used in association with other techniques in order to attain bioactive Ti devices [24–26], so that it is worth understanding the film production mechanism before different surface conditions. It was observed that bioactivity can be induced on the GD worked surfaces by the AHT technique. According to the literature [1,15], the formation of the bioactive film on Ti surface, submitted to none previous treatment, is attributed to two different and competitive chemical mechanisms in the alkali solution: (i) dissolution of the native titanium oxide layer and (ii) hydration of metallic Ti beneath the oxide layer. In both cases $HTiO_3^-$ is formed, which in association with the alkali solution ions, promotes the growing of the sodium hydrogen titanate, which will convert into sodium titanate after heat treatment. In this work, sodium titanate formed on Ti after AHT was generated in greater amount (i.e., a thicker film) than on the hydrogenated and nitrided samples. Moreover, in spite of the presence of titanium oxide in great amount, sodium titanate was not produced on the GD oxidized surface (Figs. 1b and 2). It is well known that Ti has high

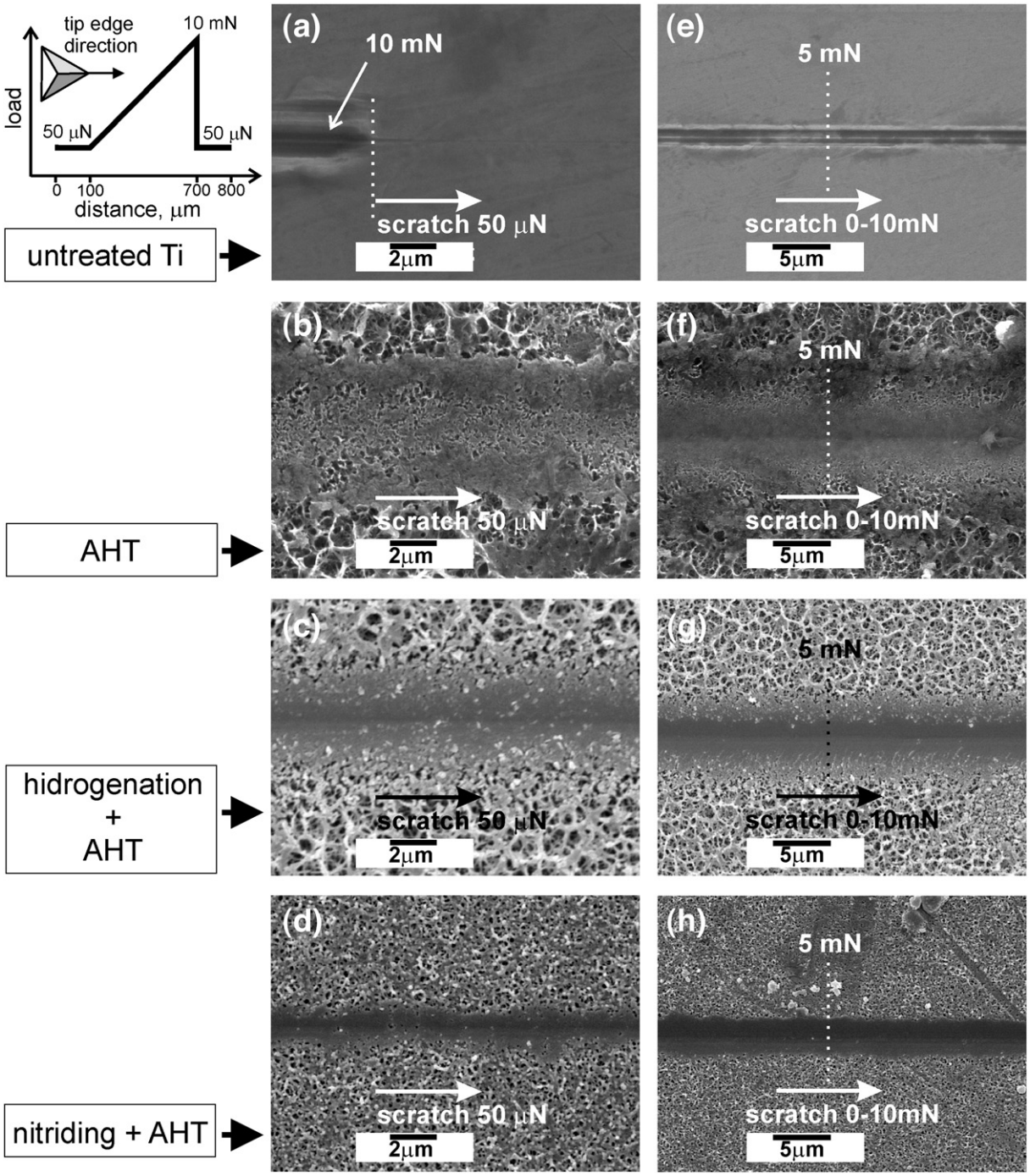


**Fig. 5.** Micrographs (SEM) of nanoscratch tracks produced on untreated Ti, AHT film on Ti and AHT films on GD worked Ti. From (a) to (d): 50 μN constant load. From (e) to (f): ramping load in the middle region of 5 mN. The inset in the upper left corner indicates the load progress during scratching.

chemical affinity to oxygen and nitrogen, more intensely to the former [27], and hydrogen is the fastest diffusing element in Ti, undergoing precipitation above a critical concentration [28,29]. Thus, the availability of metallic Ti at the surface decreases with the more thermodynamic favorable GD treatments, from hydrogenation to nitriding to oxidizing. The sodium titanate film thickness decreased in the same order. Thus, from our results we believe that hydration of metallic Ti is the predominant mechanism to sodium titanate production, because the presence of hydrides, nitrides and oxides precipitates is not favorable to the film growing.

The growing of sodium titanate films allowed the hydrogenated and nitrided surfaces to present positive *in vitro* bioactivity results in the SBF assays. Studies conducted by Takadama et al. [18] and Yamaguchi et al. [16] reported that HA starts nucleating inside the mesh structure of the bioactive film, which can also be inferred from Fig. 3. The reduction in the film thickness on the GD worked samples means reduction in amount and in the sodium titanate available to induce the HA nucleation, according to the mechanism described by [1,2]. Consequently, the *in vitro* bioactivity degree is reduced as well, varying from an effective HA layer on the Ti submitted only to AHT, to none nucleation on the oxidized sample.

It is well known that the tribo-mechanical response of coatings is dependent of substrate properties [20,30]. In the present study it was verified that the AHT film has its nanoscratch resistance decreased after GD processes, even for nitrided surfaces. As above cited the AHT film growing depends on metallic Ti availability. Compared to the film

on untreated titanium the substrate is reached in the scratch tests at loads 50% and 90% lower for the films on hydrogenated and nitrided surfaces, respectively. Consequently, the improvement of substrate mechanical properties promoted by GD is a competitive process with the AHT film growing. In summary, for biomedical purpose the GD processes on Ti do not improve at same time the osseointegration capability and the tribo-mechanical responses of the AHT Ti modified surfaces.

## 4. Conclusions

Our results for Ti submitted to DC–GD processes with the aim to obtain bioactive surfaces and improve tribo-mechanical response of AHT films allow concluding that:

a) The hydrogenation, nitriding or oxidizing by GD did not induce bioactivity in the SBF studied soaking periods. We attributed this to the low ion energies supplied by the GD processes that do not generate adequate chemical condition (hydroxyl formation) to surface calcium phosphate precipitation.
b) Untreated Ti showed high *in vitro* bioactivity after AHT by the formation of a hydroxyapatite layer on its surface. However, the film presents low tribo-mechanical response in comparison to the Ti substrate. The film hardness is ~0.02 GPa and the critical nanoscratch resistance is ~5.5 mN.
c) AHT films grown on previously GD worked surfaces (hydrogenated and nitrided) have lower bioactivity degree in comparison to the untreated Ti. The tribo-mechanical response is also decreased. Both observations are attributed to the film lower thickness in comparison to the untreated Ti. AHT film did not grow on GD oxidized surface.
d) The AHT bioactivity as well as its tribo-mechanical response has dependence on metallic Ti availability at surface during film growing in alkali environment, since the AHT film thickness reduces in the presence of hydrides, nitrides and oxides.

Further studies with XPS and FTIR techniques are in progress, aiming the best understanding of the chemical conditions at the GD worked surfaces.

## Acknowledgements

The authors are grateful to Centro de Microscopia Eletrônica/UFPR for the SEM and EDS facilities, to Laboratório de Materiais Biocompatíveis/UFPR for the bioactivity tests facilities, and the Brazilian Agency CNPq for financial support.

## References

[1] X. Liu, P.K. Chu, C. Ding, Mater. Sci. Eng. R 47 (2004) 49.
[2] T. Kokubo, H.M. Kim, M. Kawashita, Biomaterials 24 (2003) 2161.
[3] X. Liu, R.W.Y. Poon, S.C.H. Kwok, P.K. Chu, C. Ding, Surf. Coat. Tech. 191 (2005) 43.
[4] M.F. Maitz, R.W.Y. Poon, X.Y. Liu, M.T. Pham, P.K. Chu, Biomaterials 26 (2005) 5465.
[5] Y. Xie, X. Liu, A. Huang, C. Ding, P.K. Chu, Biomaterials 26 (2005) 6129.
[6] I. Braceras, J.I. Alava, L. Goiketxea, M.A. de Maeztu, J.I. Onate, Surf. Coat. Tech. 201 (2007) 8091.
[7] P.K. Chu, Surf. Coat. Tech. 201 (2007) 5601.
[8] P. Soares, A. Mikowski, C.M. Lepienski, E. Santos Jr., G.A. Soares, V. Swinka Filho, N.K. Kuromoto, J. Biomed. Mater. Res. B 84 (2008) 524.
[9] G.B. de Souza, C.E. Foerster, S.L.R. da Silva, F.C. Serbena, C.M. Lepienski, C.A. dos Santos, Surf. Coat. Tech. 191 (2005) 76.
[10] T. Kokubo, H. Takadama, Biomaterials 27 (2006) 2907.
[11] W.C. Oliver, G.M. Pharr, J. Mater. Res. 19 (2004) 3.
[12] M. Delfino, J.A. Fair, D. Hodul, J. Appl. Phys. 71 (1992) 6079.
[13] S. Ettaqi, V. Hays, J.J. Hantzpergue, G. Saindrenan, J.C. Remy, Surf. Coat. Tech. 100–101 (1998) 428.
[14] C.-W. Chang, J.-D. Liao, H.-J. Chen, C.S.F. Chang, S.-M. Chiu, Thin Solid Films 515 (2006) 122.
[15] H.M. Kim, F. Miyaji, T. Kokubo, T. Nakamura, J. Biomed. Mater. Res. 32 (1996) 409.
[16] S. Yamaguchi, H. Takadama, T. Matsushita, T. Nakamura, T. Kokubo, Key Eng. Mater. 396–398 (2009) 361.
[17] S. Nishiguchi, T. Nakamura, M. Kobayashi, H.M. Kim, F. Miyaji, T. Kokubo, Biomaterials 20 (1999) 491.
[18] H. Takadama, H.M. Kim, T. Kokubo, T. Nakamura, J. Biomed. Mater. Res. 57 (2001) 441.
[19] T. Kokubo, H.M. Kim, M. Kawashita, T. Nakamura, J. Mater. Sci.-Mater. M. 15 (2004) 99.
[20] A.C. Fischer-Cripps, Nanoindentation, Springer-Verlag, New York, 2004.
[21] T.Y. Tsui, G.M. Pharr, J. Mater. Res. 14 (1999) 292.
[22] R. Saha, W.D. Nix, Acta Mater. 50 (2002) 23.
[23] J.F. Ziegler, J.P. Biersack, U. Littmark, The Sttopping and Ranges of Ions in Solids, Pergamon Press, New York, 1978.
[24] L. Josánová, F.A. Müller, A. Helebrant, J. Strnad, P. Greil, Biomaterials 25 (2004) 1187.
[25] M. Takemoto, S. Fujibayashi, M. Neo, J. Suzuki, T. Matsushita, T. Kokubo, T. Nakamura, Biomaterials 27 (2006) 2682.
[26] A. Raknggarm, Y. Miyashita, Y. Mutoh, J. Mater. Sci.: Mater Med 19 (2008) 1953.
[27] G. Lütjering, J.C. Williams, Titanium, second ed.Springer-Verlag, Berlin, 2007.
[28] S.K. Yen, Corros. Sci. 41 (1999) 2031.
[29] C.Q. Chen, S.X. Li, Mat. Sci. Eng. A-Struct. 387–389 (2004) 470.
[30] C.M. Lepienski, C.E. Foerster, in: H.S. Nalwa (Ed.), Encyclopedia of Nanoscience and Nanotechnology, v. 7, American Scientific Publishers, USA, 2003, p. 1.